Hindawi
Geofluids
Volume 2022, Article ID 1523287, 18 pages
https://doi.org/10.1155/2022/1523287

WILEY | Hindawi

Research Article

Investigation of Non-Newtonian Characteristics of Water Flow in Micro-/Nanochannels and Tight Reservoirs

Heying Ding,[1] Fuquan Song,[1] Xiao Hu,[2] Yeheng Sun,[3] and Weiyao Zhu[4]

[1]*School of Petrochemical and Environment, Zhejiang Ocean University, Zhoushan, Zhejiang 316022, China*
[2]*Key Laboratory of Fluid Transmission Technology of Zhejiang Province, Zhejiang Sci-Tech University, Hangzhou, Zhejiang 310018, China*
[3]*Exploration and Development Scientific Research Institute of Shengli Oilfield Branch of Sinopec, Dongying 257015, China*
[4]*Civil and Resource Engineering School, University of Science and Technology Beijing, Beijing 100083, China*

Correspondence should be addressed to Fuquan Song; songfuquan@zjou.edu.cn

Received 15 March 2022; Revised 24 May 2022; Accepted 27 May 2022; Published 28 June 2022

Academic Editor: Chao-Zhong Qin

Copyright © 2022 Heying Ding et al. This is an open access article distributed under the Creative Commons Attribution License, which permits unrestricted use, distribution, and reproduction in any medium, provided the original work is properly cited.

The characteristic scale of pore flow in tight reservoirs is generally in the range of 0.1 μm to 1 μm, which shows the obvious micro- and nanoscale effect. The traditional oil and gas seepage theory cannot accurately describe the flow law of liquid in the micro- and nanopores. The determination of seepage characteristics is crucial to the development, layout, and prediction of tight oil. Therefore, a non-Newtonian fluid model is established to discuss the flow characteristics of confined liquid in the heterogeneous pores of microtubules and reveal the nonlinear seepage law of water in micro- and nanochannels and tight reservoirs. Based on the characteristics of non-Newtonian fluid of confined fluid in micro- and nanospace, the flow model of non-Newtonian fluid under the action of shear stress was deduced. The flow velocity variation of liquid in micro- and nanochannel and dense core was analyzed, and the flow rate of water was less than that predicted by macro theory. According to the flow experiment of water in micro- and nanochannels, the flow model of power-law non-Newtonian fluid was verified. At the same time, through the flow experiment of water in the dense rock core, the non-Newtonian model was used for nonlinear fitting, and the non-Newtonian power-law parameters and average pore radius were obtained, which verified the effectiveness of the non-Newtonian flow model.

1. Introduction

Driven by the micromechanical systems (MEMS) and microfluidic technology, the microchannel has become a common microdevice, which is widely used in fluid mechanics and microfluidic heat transfer. Researchers have conducted in-depth research on the applicability of the continuous media hypothesis and micro- and nanoscale flow[1]. Therefore, it is necessary to further understand the transmission phenomenon and mechanism of liquid in micro- and nanochannels, explore a new theoretical model to understand the flow state of fluid in microchannels, and study the occurrence state of fluid in micropores of tight reservoirs combined with Navier-Stokes (N-S) equation. The seepage law of water in microscale pores is analyzed to improve the understanding of the flow and transmission characteristics of fluid in the micro- and nanochannels [2]. At present, the scale larger than 1 mm is macroscale, and the scale of 1 nm to 1 mm is micro- and nanoscale. The study of fluid flow in micro- and nanoscale began in the 1980s. Ho and Tai [3] and Gal-el-Hak [4] were used as the representatives to introduce the observed microscale effects in detail through experimental studies.

1.1. Research Status of Liquid Flow in Micro- and Nanochannels

1.1.1. Liquid Flow in Micro- and Nanochannels. The classical fluid mechanics theory is based on the continuum hypothesis. When the characteristic scale decreases from micron to

nanometer, the applicability of the continuum hypothesis becomes more obvious [5]. There are many experiments on the flow law of liquids conforming to the N-S equation in the microscale channel. The fluids used are silicone oil, deionized water, distilled water, and nonpolar organic liquids. The flow experiments are conducted in different microchannel scales and cross-sections. The molecular structure of the liquid will affect the flow process, and the Reynolds number can be used as the basis for determining the nonlinear flow. Therefore, it is concluded that the flow law conforms to the macroscopic fluid mechanics theory. Table 1 summarizes the experiments conforming to the N-S equation. The studies on the micro- and nanoscale single-phase liquid flow includes the analysis of the macrofluid law, the comparison of the experimental measurement values, and the traditional theoretical value. The micro- and nanochannels with different materials and diameters are used for research. The results show that there is no microscale effect when the fluid passes through the microchannel with a diameter greater than 10 μm, which is consistent with the classical fluid mechanics theory. The critical Reynolds number (Re) of laminar flow to turbulent flow is consistent with the theoretical value.

Some studies have also shown that due to the small pore size of porous media, there is a deviation of liquid flow from classical fluid mechanics in micro- and nanoscale channels, which is attributed to the microscale effect [17, 18], as shown in Table 2. The main reason is that the channel below 10 μm is affected by the electroosmotic coupling, and the fluid has the slip phenomenon and compression effect in the micro- and nanochannel flow. The micro- and nanoscale flow has the characteristics that are different from those in the traditional flow [19, 20]. The factors that are originally ignored in the macroflow become important, which leads to the deviation of the experimental results from the traditional theoretical value: (1) The microchannel materials used in the experiment are different, and the measured results are also different. When the microchannel used in the experiment is smooth and the surface roughness is small, the measured value is basically consistent with the traditional theoretical value. When the roughness of the microchannel increases, the friction force inside the microchannel is strengthened, and the measured friction coefficient is higher than the theoretical value. (2) Different pipe diameters of fluid flow will affect the characteristics of fluid flow at low speed in microtubules. At the lower Re, the experimental value is in good agreement with the traditional theoretical value. When the Re increases and the pipe diameter decreases, the liquid begins to show the nonlinear characteristics. The experimental value is gradually greater than the theoretical value, and the degree of deviation from the classical theoretical value increases with the decrease of the inner diameter of the microtubule. When the pipe diameter is small enough, the measured value of flow resistance is less than the traditional theoretical value. (3) Different fluids were selected in the experiment, and the experimental results were also different. The flow characteristics and viscosity of different fluids are different, resulting in the change of Re from laminar flow to turbulent flow, which makes the measured and theoretical values deviate. (4) The cross-sections of the microchannel selected in the experiment are circular, trapezoidal, rectangular, and square. The effects of the inlet section of different cross-sections are different, which affects the effect of the full flow of the fluid in the microchannel and thus causes the errors in the measured fluid resistance.

At present, the inner diameter of the microchannel measured in the microscale experiment is in the order of 100 nm to 100 μm, and the existing macroscopic technical means cannot be used. Secondly, the microscale flow study is increasingly concerned about the physical phenomena in the "limit" state. Therefore, the higher requirements are put forward to create physical models and experimental observation techniques that meet the requirements, which is the focus and direction of future research.

1.1.2. Study on the Seepage Characteristics of Water in the Micro- and Nanochannels. Kandlikar [29] showed that as the channel size decreased to the microscale, the flow of water in the microchannel was limited and exhibited the obvious nonlinear behavior. Fang [30] introduced the research progress of nanowater channel. By reducing the radius of the pipe through the atoms on the inner pressure carbon pipe, the hydrogen bond between water molecules and water chains was broken, and the flow in the carbon pipe was greatly reduced, which was no longer in line with the characteristics of Newtonian fluid. When the characteristic scale of the channel drops to the nanometer, the effect of hydrodynamic boundary conditions on the velocity distribution of liquid is dominant, and the velocity distribution is nonlinear near the solid surface, which is caused by the limitation of liquid flow in the micro- and nanospace [31]. Yang and Fang [32] studied the power-law dependence of the slip length of the hydrophilic surface in the microchannel on the shear rate through molecular dynamics simulation. Shirai and Yoshida [33] used the nano-X-ray diffraction device to study the water in the nanochannel. Because the liquid is limited in a narrow space, the hydrogen bond is stronger, and the density of water is larger, so that the viscosity increases, the proton transfer becomes faster, and the movement of water molecules is limited. Finally, the proton functional groups affect the change of liquid properties in the nanochannel, which cannot present the characteristics of Newtonian fluid. Cheng et al. [34] considered the influence of non-Newtonian rheological effect and solved the N-S equation to simulate the fluid flow in the microchannel to determine the non-Darcy flow in the microchannel under low pressure gradient.

When Ling et al. [35] studied the flow of deionized water in the micro- and nanochannels, the flow rates of water in hydrophilic surface pipelines and hydrophobic surface pipelines were measured, respectively. Due to the surface slip in the hydrophobic pipeline, the flow rate increased significantly, and there was a nonlinear relationship between pressure and flow rate. The roughness of the surface of the microchannel in the hydrophilic surface pipeline had little effect, and the pressure-flow characteristics conformed to the N-S equation. Under the influence of pipe roughness at the micro- and nanoscale, Yu et al. [36] carried out the

Table 1: Flow experiment in microcircular channel according to the N-S equation.

Fluid	Microtubule scale	Cross section	Re	Document
Silicone oil	11.8-50 μm	Circular	<10	Makihara et al. [6]
Deionized water	8-40 μm	Circular	<64	Jiang et al. [7]
Deionized water	25-35 μm	Circular	130-330	Aniskin et al. [8]
Distilled water	27-63 μm	Trapezoid	<600	Flockhart and Dhariwal [9]
Nonpolar organic liquid	25 μm	Circular	<8	Li et al. [10]
Distilled water	12-150 μm	Circular	8-2300	Judy et al. [11]
Methanol, isopropanol	79.9-166.3 μm 100.25-205.3 μm	Square/trapezoid/circle	About 64	Li [12]
Deionized water	50-100 μm	Circular	90-800	Salman et al. [13]
Deionized water	16-30 μm	Circular	<4	Xu et al. [14]
Deionized water	172-520 μm	Circular	800-1000	Bucci et al. [15]
Deionized water	30-326 μm	Circular	>300	Celeta et al. [16]

Table 2: Flow experiment deviating from the N-S equation in microcircular channels.

Fluid	Microtubule scale	Cross section	Re	Experimental result	Document
Water isopropanol	20-75 μm	Circular	20-2000	Flat	Judy et al. [21]
Water	128.76-179.8 μm	Rectangle	1700-2000	On the high side	Li et al. [22]
Deionized water	300 μm	Trapezoid	1-30	Flat	Jiang et al. [23]
Deionized water	128.76-179.8 μm	Circular	500-2000	On the high side	Li [12]
Deionized water	133-343 μm	Rectangle	50-4000	Flat	Peng et al. [24]
Deionized water	2-5 μm	Circular	<4	On the high side	Xu et al. [14]
Deionized water	2-10 μm	Circular	20-4000	Flat	Jiang et al. [25]
Aviation kerosene crude oil	2-5 μm	Circular	10-2000	Flat	Wang et al. [26]
Deionized water	<10 μm	Circular	50-4000	Flat	Song and Yu [27]
Different ionic solution	<44.5 μm	Circular	800-4200	Flat	Chen [28]

experiments in a circular superhydrophobic micropipe in the laminar region. By measuring the pressure drop and volume flow rate of water, it was found that water showed slip characteristics in the flow process. Due to the influence of large surface roughness, the water pressure in the micropipe increased with the increase of volume flow rate. Qu and Song [37] used the deionized water; the experiments were conducted in the microchannels with the inner diameters of 50 μm, 75 μm, and 100 μm, respectively. With the decrease of the inner diameter of the microchannel, the movement of the fluid was limited under the same pressure, and the boundary slip behavior between the fluid and the wall was observed, which indicates that the slip boundary will have an important influence on the liquid flow in the microchannels and nanochannels. Jiang et al. [38] and Song et al. [39] studied the flow experiments of the deionized water at micro- and nanoscales, which showed that the superhydrophobic surface was more prone to slip at micro- and nanoscales. Due to the influence of roughness and surface energy, the liquid flow would not conform to the assumption of continuous medium, showing nonlinear characteristics.

These literatures studied the water flow characteristics in the micro- and nanochannels, such as the spatial distribution of liquid, velocity distribution, and slip length and analyzed the generation of nonline in the microchannels.

1.2. Study on Nonlinear Seepage Characteristics of Liquid in Tight Reservoir. With the increasing development of the global economy, oil consumption has increased year by year, and the development of conventional oil and gas fields is difficult to meet the demand. Tight reservoirs have become a very important goal of the modern oil industry [40–42]. It is generally believed that continuous reservoirs without large-scale and long-distance transportation in tight reservoirs are tight reservoirs, such as sandstone and carbonate, with porosity less than 10% and permeability less than 0.1 mD [43]. According to the U.S Department of Energy Information, the recoverable resources of continental tight oil technology in China are 44.8×10^8 t, and the production capacity of continental tight oil in China reached 155.3×10^4 t in 2016 [44–47]. In recent years, the significant progresses have been made in the exploration and development of continental tight oil. By the end of 2018, the production capacity of continental tight oil in China has been 315.5×10^4 t, with an annual output of about 105×10^4 t in 2018. It is expected that the production capacity of tight oil in 2035 will reach 1500×10^4 t, and the exploitation potential is huge [48, 49], which indicates that tight oil is essential to increase oil reserves and production in China in the future.

In recent years, a large number of studies have been carried out on the fluid characteristics in tight reservoirs. Most

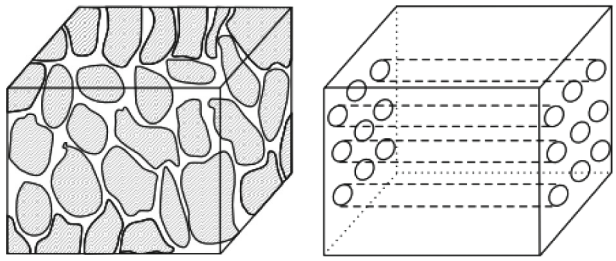

Figure 1: Capillary bundle model [54].

of the seepage mechanisms and seepage models of low-permeability and ultra-low-permeability reservoirs are used in the experimental study of tight reservoirs. However, the reasons for the non-Darcy characteristics generated by the seepage of porous media are still unclear. The main reason is that the experimental study of the seepage characteristics of low-permeability porous media in tight reservoirs is mostly based on a macroperspective, and the pores in porous media are disorderly, and it is difficult to quantitatively characters [50, 51]. As the effects of viscosity, surface force, and interface slip at the micro- and nanoscales become obvious, the fluid flow has different fluid characteristics compared with the macroscopic aspect. Therefore, it is essential to study the fluid flow characteristics at the micro- and nanoscale. Since the continuum hypothesis model cannot accurately analyze the fluid flow characteristics at the micro- and nanoscale, the molecular dynamics method simulates the molecular motion system with the help of classical mechanics and calculates the relevant physical quantities through integral calculation to describe the fluid motion law at the micro- and nanoscale. The molecular dynamics simulation is used to predict the changes of water viscosity and slip length with the diameter of carbon nanochannels [52, 53].

1.3. Relationship between Fluid in Porous Media and Microtubule Flow Model. In the tight reservoirs, the establishment of capillary bundle model based on pore characteristics is one of the commonly used physical models to characterize the porous media. The classical capillary bundle seepage model is composed of a cluster of capillary channels with equal length and different diameters, which flows along the direction of fluid [54–56]. Dullien [57] formally put forward the concept of capillary bundle model and pointed out that the pore network of actual porous media is regarded as a cluster of straight capillary bundle models with equal length and unequal diameter. The model equates the equation of flow calculated by pipeline fluid mechanics and the calculation of seepage mechanical flow, which is of great significance to the calculation of pore and seepage parameters of rock pore structure. Therefore, the model is called "classical capillary bundle seepage model," as shown in Figure 1.

In the seepage mechanics, many liquid nonlinear flow experiments are verified by capillary bundle model. For example, Purcell [58] converted the rock into a model composed of N cylindrical capillary bundles of equal length and different diameter and deduced the calculation equation of absolute permeability of rock by combining the Darcy equation and the Poiseuille equation. Liu et al. [59] assumed that the core was composed of countless capillary parallel with different pore throats. The capillary model was used to calculate the starting pressure gradient, and the nonlinear relationship between the starting pressure gradient, the starting permeability, and the flow rate was verified by the experiments.

In this study, a power-law nonlinear flow model is established for the seepage phenomenon of confined liquid in the micro- and nanoporous media. The capillary beam is used to connect the fluid flow in the microchannel and the pore of dense core, and the influence of microscale effect on the fluid flow is analyzed. The correctness of the power-law nonlinear flow model is verified, which proves that the model can explain the phenomenon of nonlinear flow theoretically. In the experiment, the pore range of liquid flow is between 50 nm and 5 μm, and the seepage experiment of water in the pores of micro- and nanochannels and tight reservoirs is conducted. The relationship between the shear rate of non-Newtonian power-law fluid, the change of pressure field, and the parameter n of nonlinear model is analyzed and verified. The error between the pore diameter of tight rock core and the measured value is less than 1% through experimental fitting, which proves that the fluid model is effective and can be used for the theoretical study of the flow law of single-phase liquid at the microscale.

2. Non-Newtonian Fluid Model of Liquid Flow at Micro- and Nanoscale

Based on the characteristics of non-Newtonian fluid of confined liquid in the micro- and nanospace, the flow phenomenon of non-Newtonian fluid in an irregular microcircular channel is studied. The characteristics of velocity field distribution and shear strain rate of non-Newtonian fluid in the channel were analyzed and then verified by the flow experiment of water in a micro- and nanochannel.

The stress-strain relationship of power-law non-Newtonian fluid can be written as

$$\tau = H\gamma^n, \tag{1}$$

where τ is the stress on the fluid, Pa; γ is the strain of the fluid, s^{-1}; H is the consistency coefficient, mpa.s; and n is the power-law parameters.

For the fluid microcircular section dL, the shear stress direction is to the left and opposite to the flow velocity v, and the stress and strain equations [60] are written, respectively, as

$$\tau = -\frac{r}{2}\frac{\mathrm{d}p}{\mathrm{d}L}, \tag{2}$$

$$\gamma = -\frac{\mathrm{d}v}{\mathrm{d}r}, \tag{3}$$

where r is the pore radius, μm.

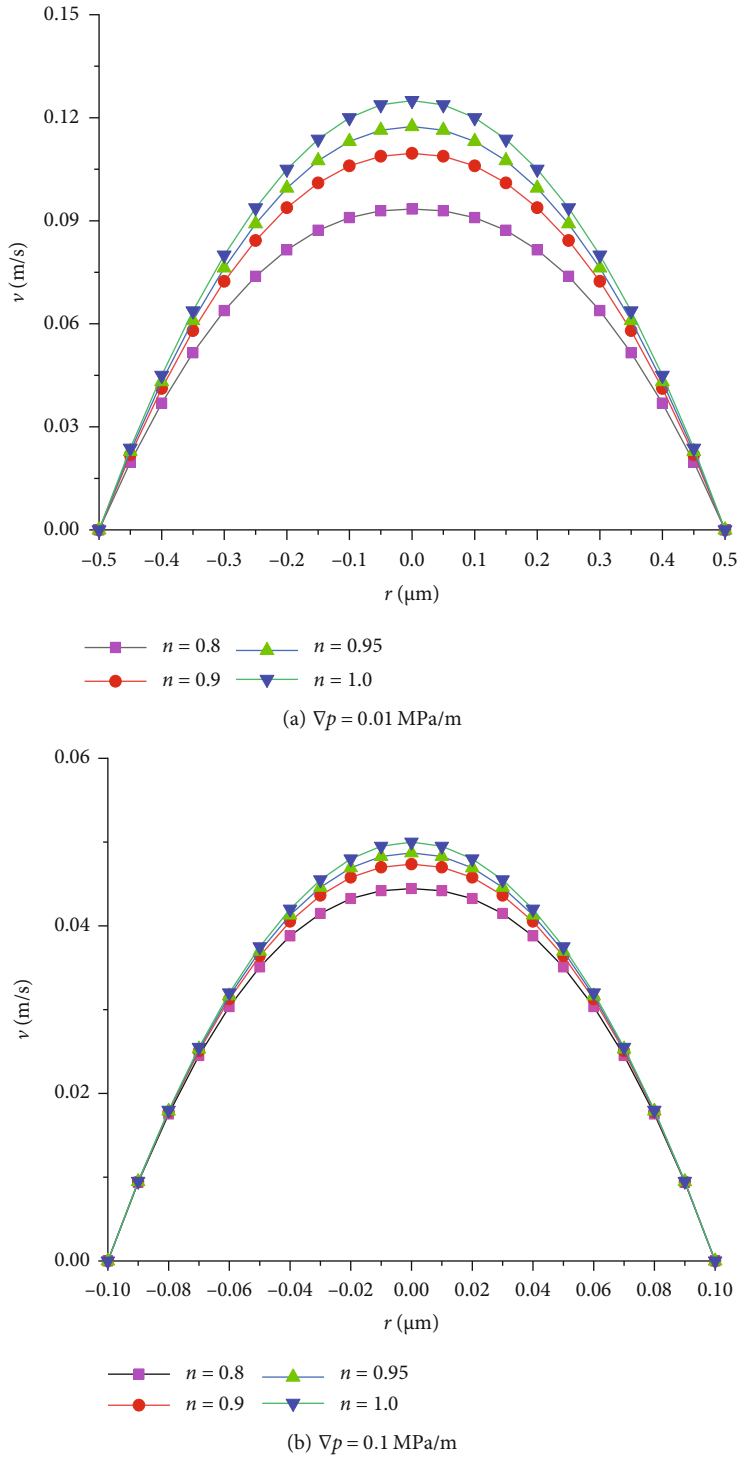

Figure 2: Profile of pipe diameter and microtubule velocity in microtubule.

Substituting Equation (2) and Equation (3) into Equation (1), we can obtain

$$-\frac{r}{2}\frac{\mathrm{d}p}{\mathrm{d}L} = H\left(-\frac{\mathrm{d}v}{\mathrm{d}L}\right)^{n}. \tag{4}$$

With the boundary condition of $v = 0$ at $r = r_0$, it is obtained that

$$v = \left[\left(-\frac{1}{2H}\frac{\mathrm{d}p}{\mathrm{d}L}\right)^{1/n} \cdot \frac{n}{n+1}\right]\left(r_0^{\,n+1/n} - r^{n+1/n}\right). \tag{5}$$

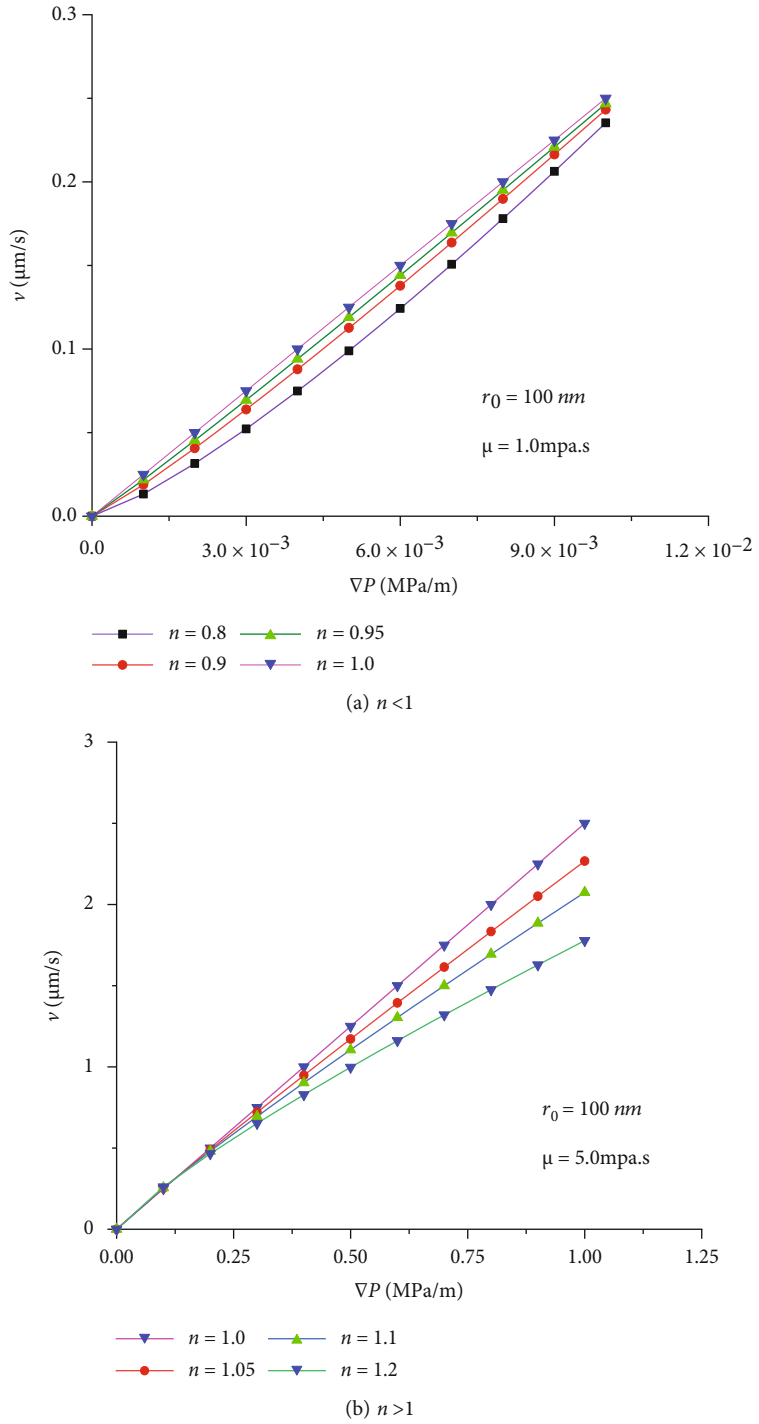

Figure 3: Relationship between liquid pressure gradient and flow velocity in micro-nanocircular channels.

The flow velocity profile of non-Newtonian fluid can be drawn by the above the equation. Assuming $r_0 = 0.5\,\mu$m and $\mu = 5$ mPa.s, under the condition of $\nabla p = 0.01$ MPa/m and 0.1 MPa/m and different micro- and nanoscale pipe diameters, we draw the relationship between pipe diameter and microtubule flow rate, as shown in Figure 2. For the different liquids, when the other conditions are the same, the flow rate of non-Newtonian fluid with pressure gradient below 0.03 MPa/m and power-law coefficient less than 1 can be calculated, as shown in Figure 2(a). When the pipe diameter decreases from micron scale to nanometer scale, increasing the driving pressure gradient can reduce the velocity gap, and the velocity distribution is close to the Newton fluid, as shown in Figure 2(b).

When the pipe diameter is reduced to the nanoscale and the driving pressure gradient is increased, the velocity gap

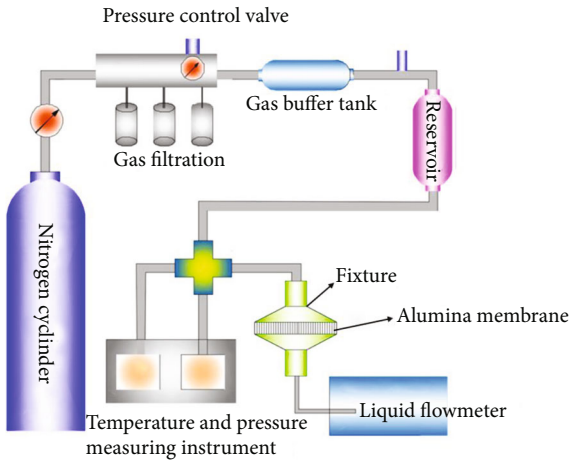

Figure 4: Micro- and nanochannel experiment system chart [63].

can be reduced and the velocity distribution is closer to Newtonian fluid, as shown in Figure 2(b).

The total flow in the microchannel is obtained by integration.

$$Q_p = \int_0^{r_0} v \cdot 2\pi r \cdot \mathrm{d}r = \left(-\frac{\pi}{2H}\frac{\mathrm{d}p}{\mathrm{d}L}\right)^{1/n}\left(\frac{n}{1+3n}\right) {r_0}^{3n+1/n}. \quad (6)$$

Therefore, the average velocity in the pipeline is written as

$$\bar{v} = \frac{Q_p}{\pi {r_0}^2} = \left(\frac{n}{1+3n}\right) {r_0}^{n+1/n}\left(-\frac{1}{2H}\frac{\mathrm{d}p}{\mathrm{d}L}\right)^{1/n}. \quad (7)$$

Through Equation (7), the relationship between the liquid pressure gradient and flow velocity in a circular channel at microscale can be obtained, as shown in Figure 3.

As can be seen from Figure 3, the relationship between fluid pressure gradient and flow velocity in nanochannels is discussed in two cases. When $n = 1$, it presents Newtonian fluid characteristics. According to the average velocity equation, there is a linear relationship between the pressure gradient and the velocity. When $n < 1$ or $n > 1$, it shows nonlinear characteristics according to the velocity equation of the fluid in the pipeline. The curve in Figure 3(a) is concave, which indicates that the difference between the velocity of confined fluid and that of Newtonian fluid is obvious under the small driving force (shear rate). When the driving force increases, the fluid velocity in the channel tends to be linear with the increase of driving force. The curve in Figure 3(b) is convex, indicating that under small driving force (shear force), the difference between the flow velocity of the fluid and that of the Newtonian fluid is small. When the driving force increases and the model parameter n increases to 1.2, the influence of the confined fluid increases, and the flow velocity in the channel deviates from the Newtonian fluid significantly. The flow velocity of the fluid in Figures 3(a) and 3(b) is smaller than that of the Newtonian fluid, which implies that the diameter, driving force, and pressure gradient are the main factors that determine the flow velocity. However, the experimental values in the micro- and nanochannel are all smaller than the theoretical values. That is, when the displacement pressure gradient in Figure 3(a) is reduced to 0.005 MPa/m, and the pressure gradient in Figure 3(b) is reduced to 0.5 MPa/m, the bending degree of the liquid flow velocity curve increases, and the nonlinear characteristics are obvious.

A large number of experimental studies show that the microscopic parameters such as reservoir physical properties, fluid properties, and the interaction of solid-liquid interface have varying degrees of influence on the nonlinear seepage of the tight reservoir, which has a certain guiding role in exploring the development of tight reservoir. The storage of crude oil in the tight reservoir is mainly concentrated in the pores of 0.1~1 μm, and the physical properties of the liquid, including crude oil, are different from those under the macroconditions [61, 62]: The flow of liquid presents the characteristics of non-Newtonian fluid, and the shear stress of non-Newtonian fluid has a nonlinear relationship with the shear rate.

For the porous media, consider that there are a large number of capillaries in the porous medium, and the diameters of the channels are not uniform. Therefore, suppose that the length of the medium is L, and the number of capillaries with radius on the cross-sectional area A is $N_i (i = 1, 2, \cdots, N)$. According to Equations (6) and (7), the total flow Q through the cross-sectional area A for the capillary bank case should be

$$Q = \sum_{i=1}^{N}\left[N_i {r_i}^{3n+1/n}\left(-\frac{1}{2H}\frac{\mathrm{d}p}{\mathrm{d}L}\right)^{1/n}\left(\frac{n\pi}{1+3n}\right)\right]. \quad (8)$$

The porosity is defined as

$$\phi = \frac{\sum_{i=1}^{N} N_i \pi {r_i}^2}{A}. \quad (9)$$

So, the seepage velocity ($v = Q/A$) can be obtained.

$$v = \left(-\frac{1}{2H}\frac{\mathrm{d}p}{\mathrm{d}L}\right)^{1/n}\left(\frac{n\phi}{1+3n}\right)\frac{\sum_{i=1}^{N} N_i {r_i}^{3n+1/n}}{\sum_{i=1}^{N} N_i {r_i}^2}. \quad (10)$$

Assuming the capillary bundle model and assuming that the average radius of capillary bundle is $\bar{r}_0$, the seepage velocity equation in a low-permeability tight reservoir can be obtained.

$$v = \frac{n}{3n+1}\phi {\bar{r}_0}^{n+1/n}\left(-\frac{1}{2H}\frac{\mathrm{d}p}{\mathrm{d}L}\right)^{1/n}. \quad (11)$$

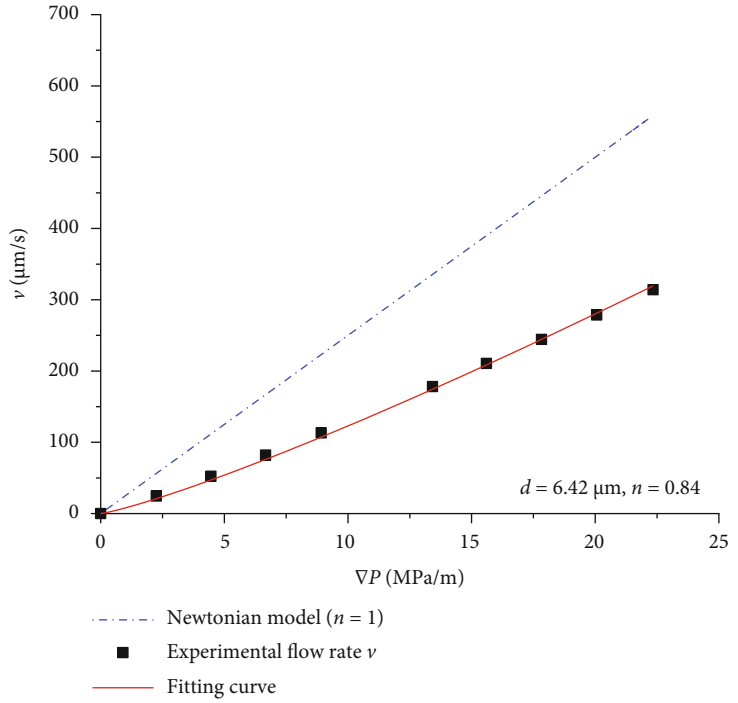

(a)

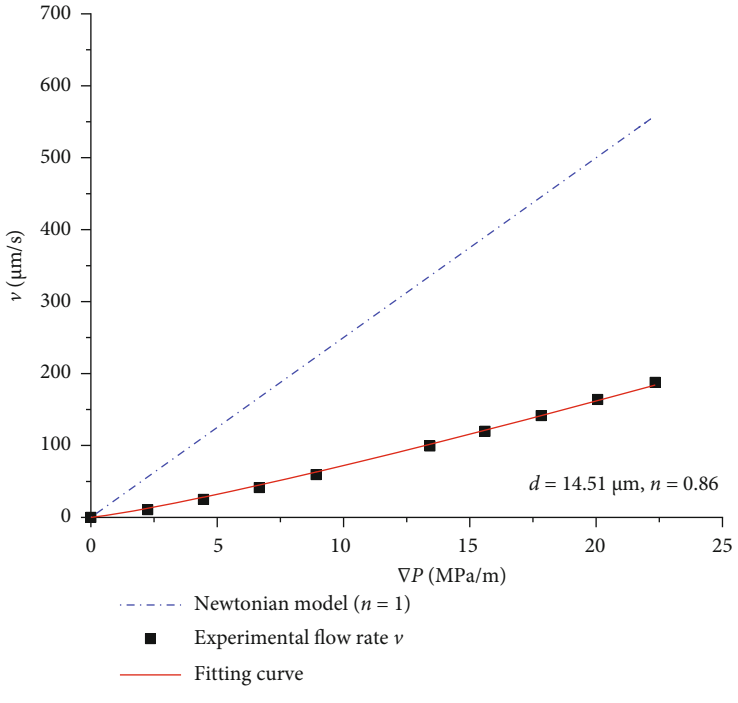

(b)

Figure 5: Continued.

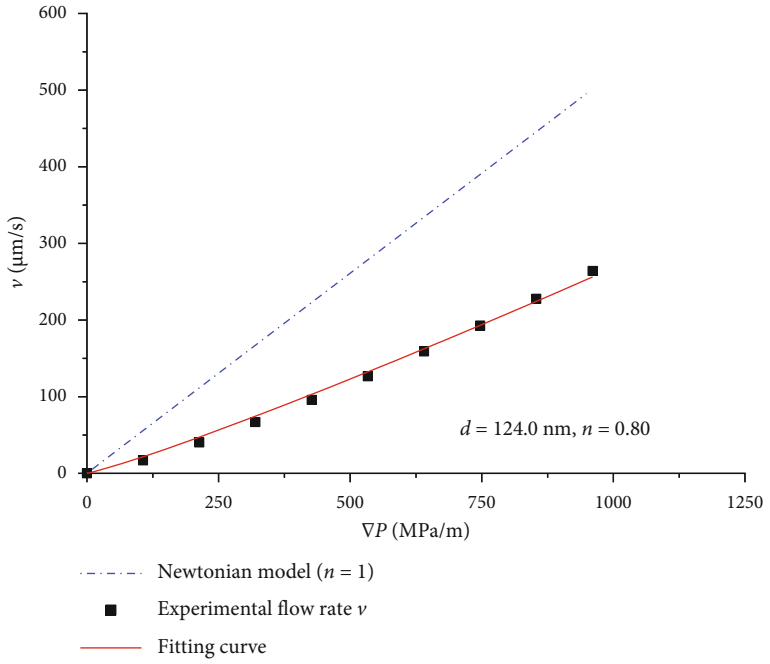

(c)

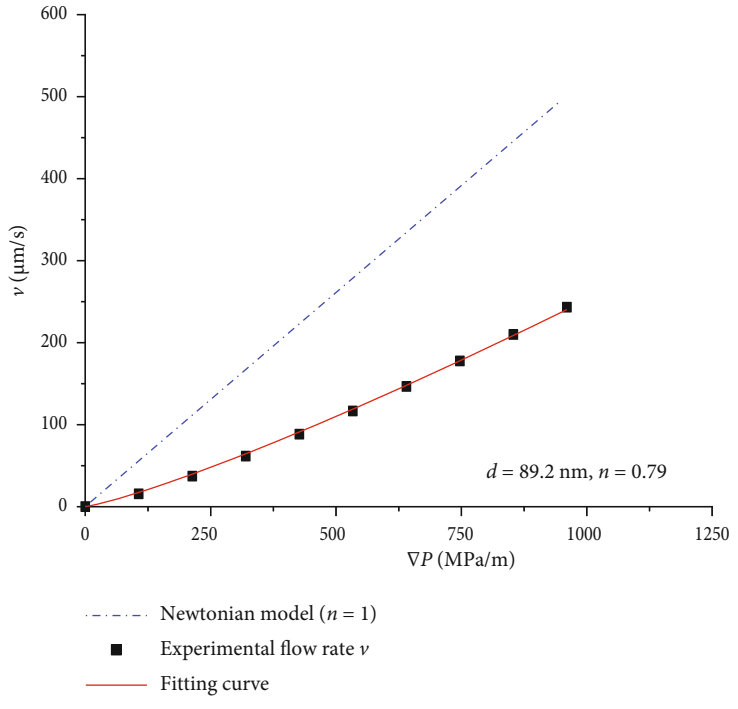

(d)

Figure 5: Continued.

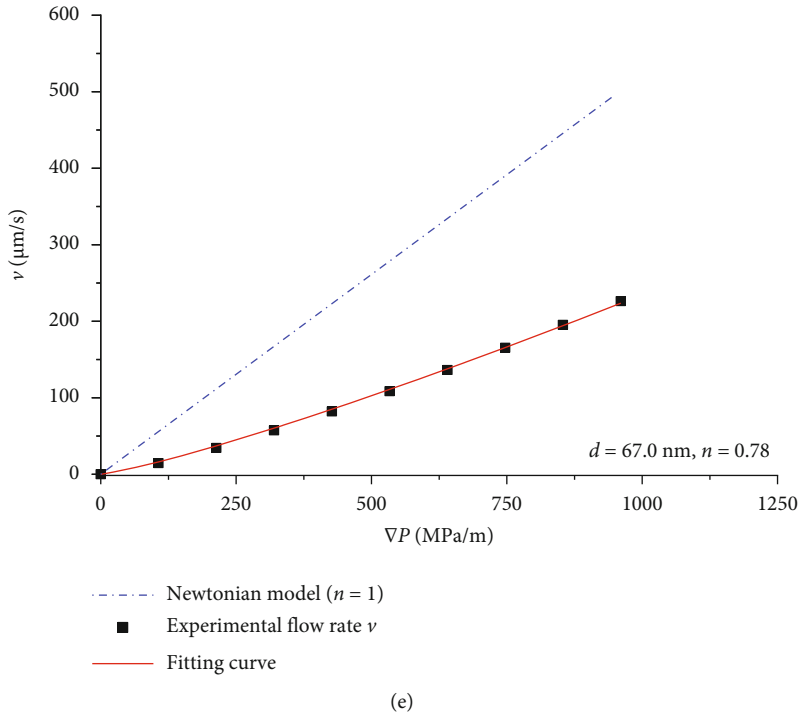

(e)

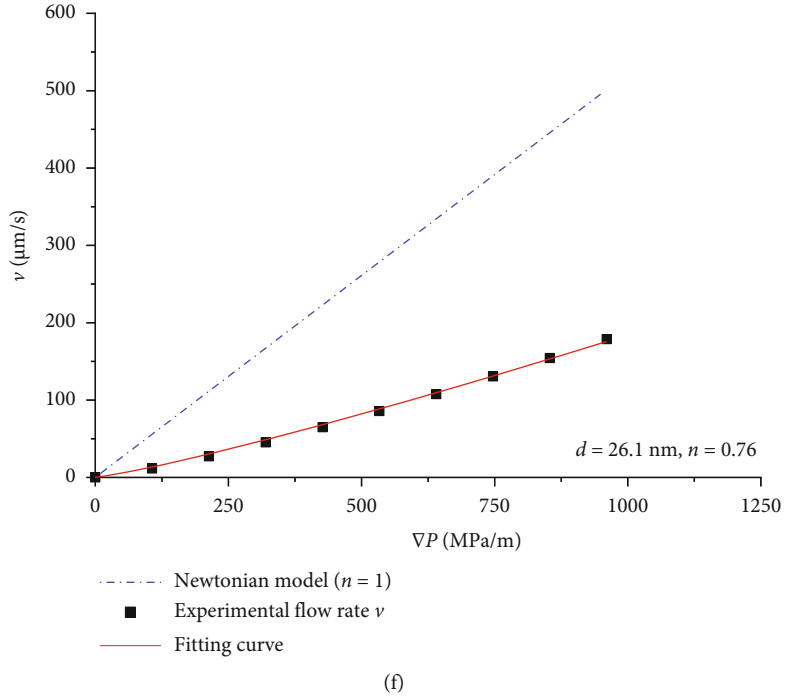

(f)

Figure 5: Experimental curves of water flow in micro- nanochannels with different diameters.

Equation (11) is converted to the form of Darcy's Law.

$$v = -\frac{k}{\mu_e}\frac{\mathrm{d}p}{\mathrm{d}L}, \tag{12}$$

where the permeability of the core is defined as

$$k = \frac{\phi \bar{r}_0^{\,2}}{8}, \tag{13}$$

and the apparent viscosity μ_e is defined as

$$\mu_e = \left(\frac{1+3n}{8n}\right)\bar{r}_0^{\,n-1/n}\left(\frac{1}{2H}\right)^{-1/n}\left(-\frac{\mathrm{d}p}{\mathrm{d}L}\right)^{n-1/n}. \tag{14}$$

Equation (12) shows that in the power-law non-Newtonian model, the apparent viscosity of the fluid is related to the intrinsic viscosity μ of the fluid, the power-law n value, the diameter of the micro-nanochannel, and

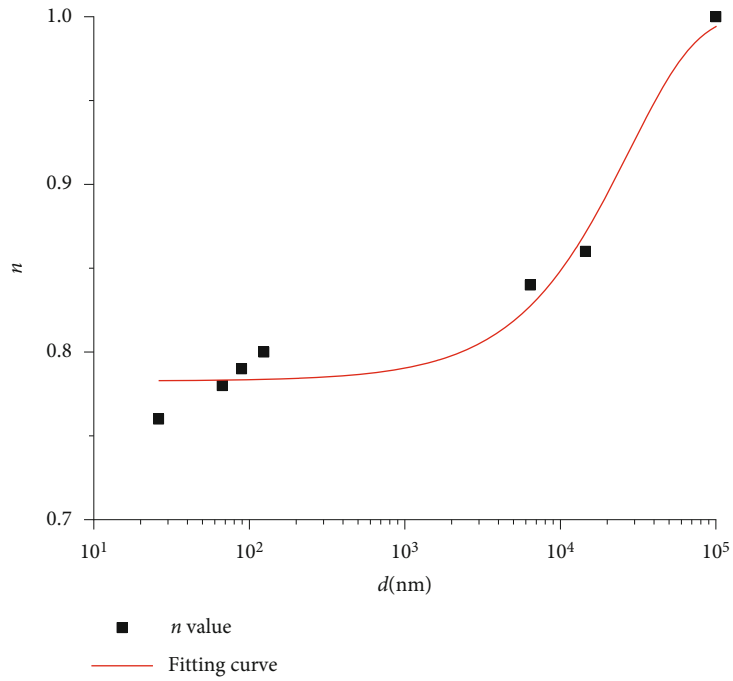

Figure 6: Nonlinear relationship between non-Newtonian parameter n value and micro-nanochannel diameter.

Table 3: Basic parameters of the experimental cores (sandstone core).

Serial number	Core Number	Length (mm)	Diameter (mm)	Porosity (%)	Permeability (mD)
1	154-1-5	50.42	24.95	17.54	0.77
2	154-7-20	51.45	24.86	13.59	0.17
3	154-8-38	51.85	24.88	18.53	0.84
4	154-8-40	51.35	24.92	15.25	0.15
	Average	51.27	24.90	16.23	0.48

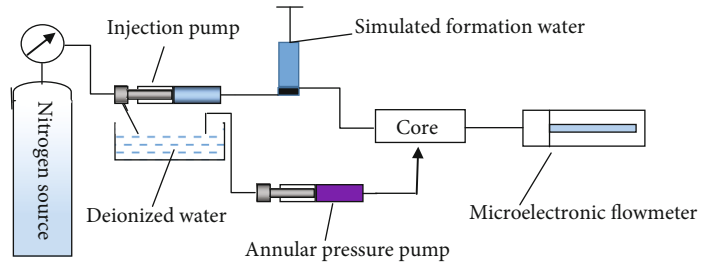

Figure 7: Flow chart of single-phase water drive experiment in tight core [50].

the pressure gradient during the displacement. Equation (14) shows that the effective permeability is related to the properties of the porous medium and the capillary radius and also to the power-law parameter n.

3. Experimental Study of Water Phase in Micro- and Nanochannel

Quartz capillary channels with pore sizes of 6.42 μm and 14.51 μm and channels in the alumina membrane with pore sizes of 124.0 nm, 89.2 nm, 67.0 nm, and 26.1 nm were selected in the experiment. The alumina membrane was purchased from Shenzhen Tuopu Fine Film Technology Company. The experimental research is conducted under the pressure difference of 0.01-0.10 MPa. The flow characteristics of deionized water are analyzed by the measurement, calculation, and fitting. The specific experimental process is shown in Figure 4, and the experimental equipment is as follows: deionized water, quartz capillaries, photoelectric displacement detector, temperature-pressure display instrument, pressure controller, nitrogen bottle, etc. The theoretical calculation method is shown in Equation (7).

3.1. Experimental Method. Due to the precision requirements of the experiment, the whole experimental process was carried out in the VS-840 U purification workbench

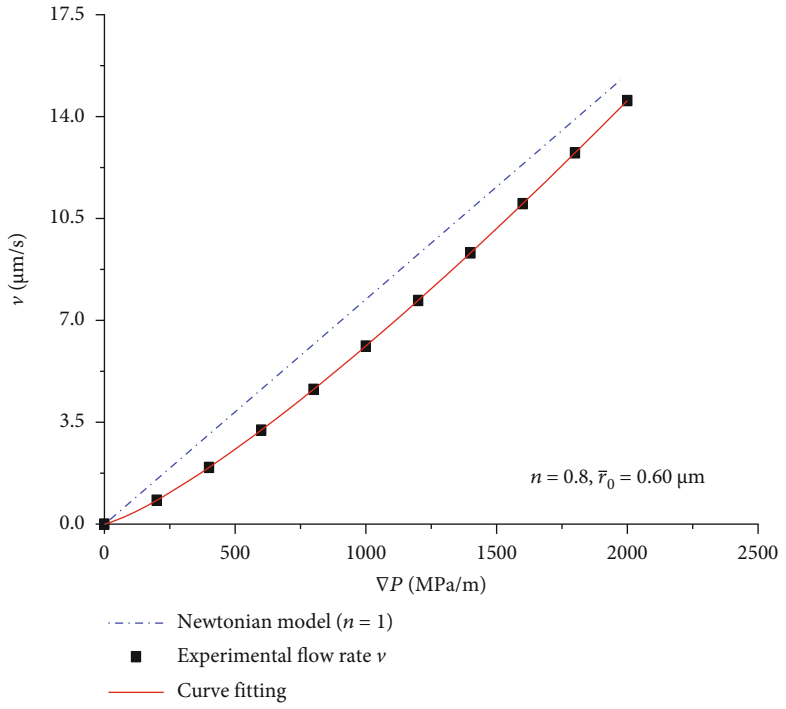

(a) Core 154-8-38

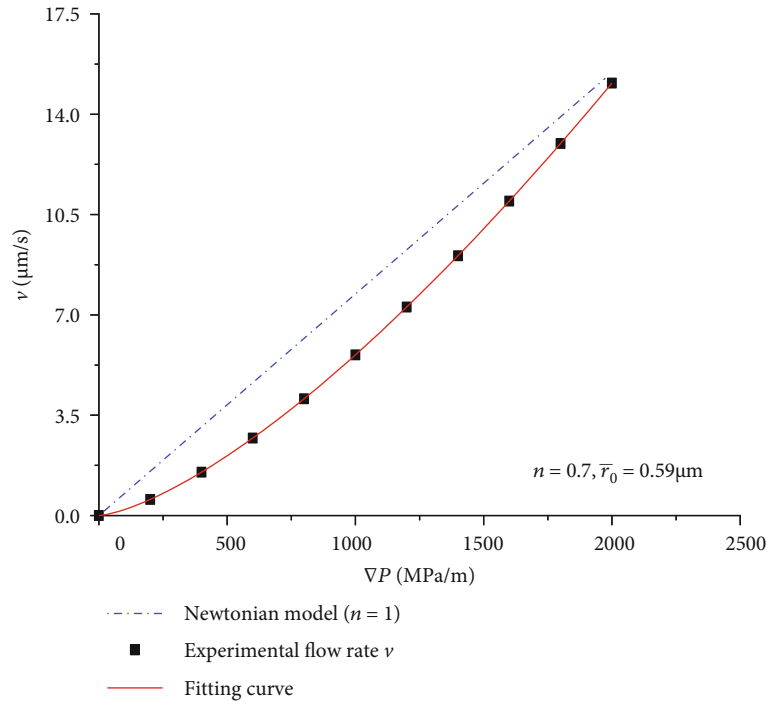

(b) Core 154-1-5

Figure 8: Continued.

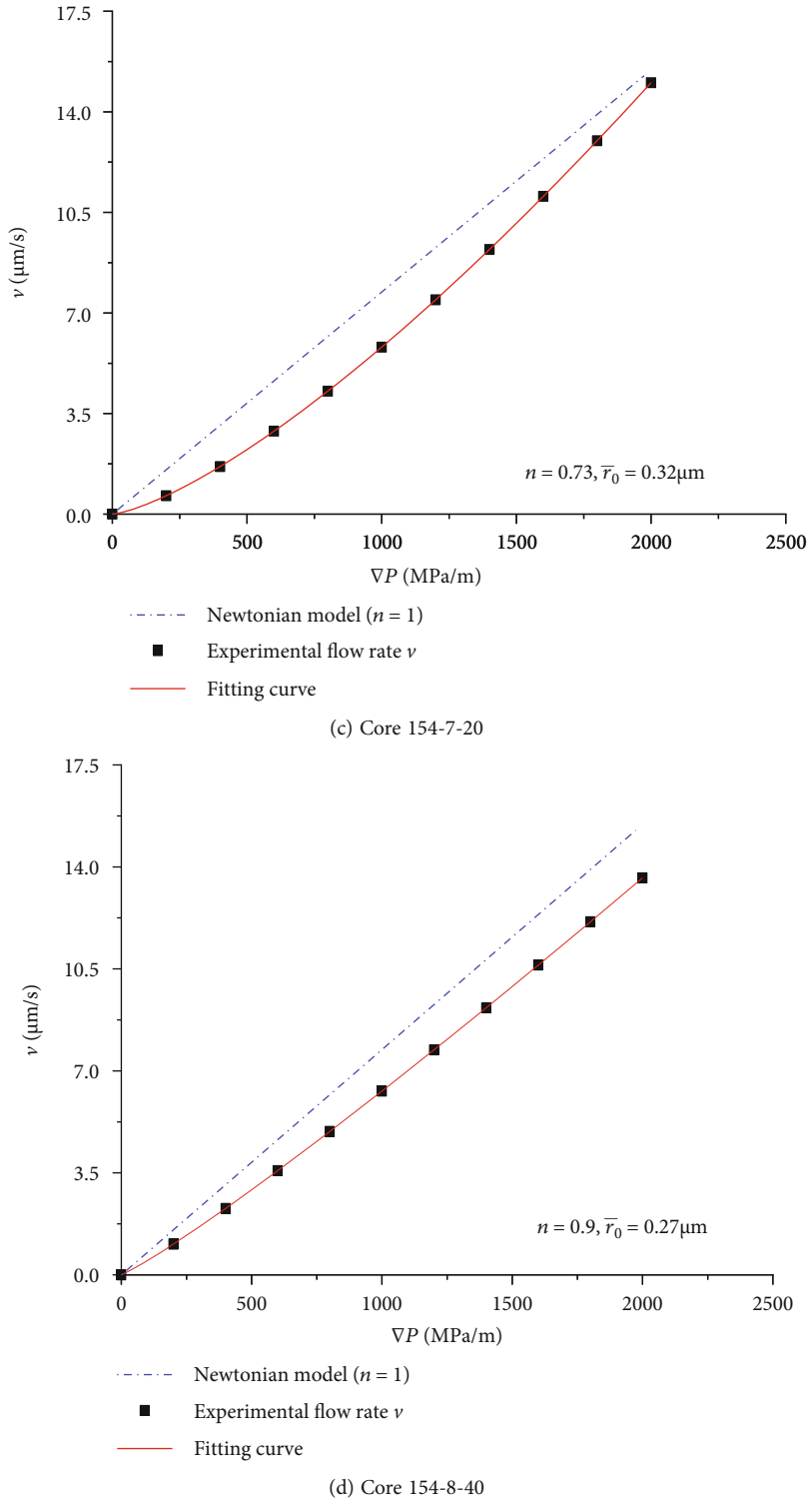

Figure 8: Nonlinear fitting of pressure gradient and water velocity in cores.

(cleanliness level 10), and the specific operation process was as follows: (1) deionized water filtered by nanomembrane and sterilized by ultraviolet light is added to the liquid tank; (2) the instruments in each part of the experiment are sealed with high-pressure resistant plastic pipes, and then, each pipeline is connected with the power supply; (3) fix and seal rubber ring of the nanofilm; (4) the nitrogen with purity of 99.99% is used to deliver pressure to the whole experimental device, and the temperature and pressure are measured by the temperature and pressure measuring instrument, and the liquid flow is measured by the liquid flowmeter; (5) continuously adjust the displacement pressure by controlling

the nitrogen source, measure the flow rate of deionized water, and conduct multiple experiments to obtain the average value to reduce the error; and (6) after the measurement, remove the alumina film and check whether it is damaged. If the film is damaged, the experimental data is invalid and needs to be retested.

3.2. Experimental Results and Analysis. According to the above experimental process and the calculation equation of the microcircular channel, the non-Newtonian velocity (Equation (7)) is used for fitting, and the results are shown in Figure 5. The experimental results of the microtubule velocity are in good agreement with the fitting curve of Newton model, and the relative error is small, which proves that the non-Newtonian fluid calculation model established in this study is suitable.

It can be seen from Figure 5 that there is the displacement pressure in the micro- and nanochannel, and the water flow is significantly less than the predicted flow rate of Newtonian fluid pipe flow under the macroscopic conditions. The water flow rate in the micro- and nanochannel increases slowly in the early stage, and the pressure increases from 2 MPa to 5 MPa. The flow rate has a large increase, and the overall trend is concave, which shows the motion characteristics of non-Newtonian fluid. When the inner diameter of the channel increases continuously, the non-Newtonian power-law coefficient n increases from 0.76 to 0.80, and with the increase of the inner diameter of the channel to the order of 10^5nm, the exponent n in the model gradually approaches 1. No matter how the aperture increases, the experimental results are less than the flow velocity calculation results obtained by the Newtonian fluid theory.

This is a seepage experiment conducted in a microscale circular channel. A layer of alumina film is laid in the circular channel, so that the surface of the pipeline is hydrophobic and the friction force on the surface of the pipeline is reduced. There is a low-density liquid layer on the hydrophobic surface, resulting in the slip phenomenon. Finally, the flow law does not conform to the Darcy flow and presents the nonlinear flow characteristics.

According to the nonlinear relationship between the diameter of micro- and nanochannels and the n value of non-Newtonian power-law coefficient, the fitting equation is obtained as follows:

$$n = 1 - 0.217 * e^{\left(-3.6*10^{-5}*d\right)}. \quad (15)$$

According to the fitting curve drawn by Equation (15), the value of n also increases with the increase of the inner diameter d of the microchannel and finally approaches 1, as shown in Figure 6.

4. Study on the Characteristics of Water Phase Seepage in Tight Cores

Through four typical cores in a tight reservoir of Sheng Li Oilfield, simulate the flow of formation water in the core, measure the flow rate of each core under different pressures, and select the equation model to fit the experimental data. The basic parameters of the cores are shown in Table 3.

Table 4: Calculation and fitting results of experimental core pore diameter.

Core number	Aperture calculation $\bar{r}_0(\mu m)$	Fitting aperture $\bar{r}_0$ (μm)
154-8-38	0.60	0.60
154-1-5	0.59	0.588
154-7-20	0.33	0.327
154-8-40	0.27	0.263
Average	0.45	0.44

Table 5: Fitting results of experimental core diameter (sandstone core).

Core number	k (mD)	$\bar{r}_0$ (μm)	n
154-8-38	0.84	0.60	0.80
154-1-5	0.77	0.59	0.70
154-7-20	0.17	0.33	0.73
154-8-40	0.15	0.27	0.90
Average	0.48	0.45	0.78

4.1. Experimental Scheme and Steps. In order to prevent the clay expansion in the core and cause the physical change of the core, the simulated formation water is used to flow in the core. The experimental water standard is the simulated formation water with salinity of 30 g/L and viscosity of 1.0 mPa.s. According to the development of tight reservoirs, the main components are $CaCl_2$ (20 g/L) and $NaHCO_3$ (10 g/L).

The experimental process is shown in Figure 7. The experimental steps are as follows: (1) using BH-3 type core evacuation pressure saturation experimental device, after the core is evacuated for 5 hours, the pressure is 30 MPa, and the simulated formation water is saturated for 48 hours; (2) connect the pipeline of the experimental device and put the core into the core holder; (3) open the nitrogen bottle, turn on the pressure change pump and injection pump, and inject the simulated formation water at a constant pressure (1 MPa-10 MPa) at the inlet end. Under each displacement pressure, the confining pressure applied by the core holder is 5 MPa higher than that of the core holder; (4) measure the flow at the outlet end with a microtubule flowmeter, and record the flow value under each displacement pressure after the flow is stable; (5) replace the core and repeat the above steps; and (6) put the rock core into the drying oven, dry it continuously at 25°C~45°C for 48 hours, and cool it to room temperature for later use.

4.2. Experimental Results and Analysis. Through the non-Newtonian model (Equation (12)), the water flow velocity and pressure gradient in four cores are nonlinear fitted to obtain the n value and $\bar{r}_0$ value. As shown in Figure 8 (the water viscosity in the experiment is 1.0 mPa.s), the flow rate curve with pressure gradient shows a concave trend as a

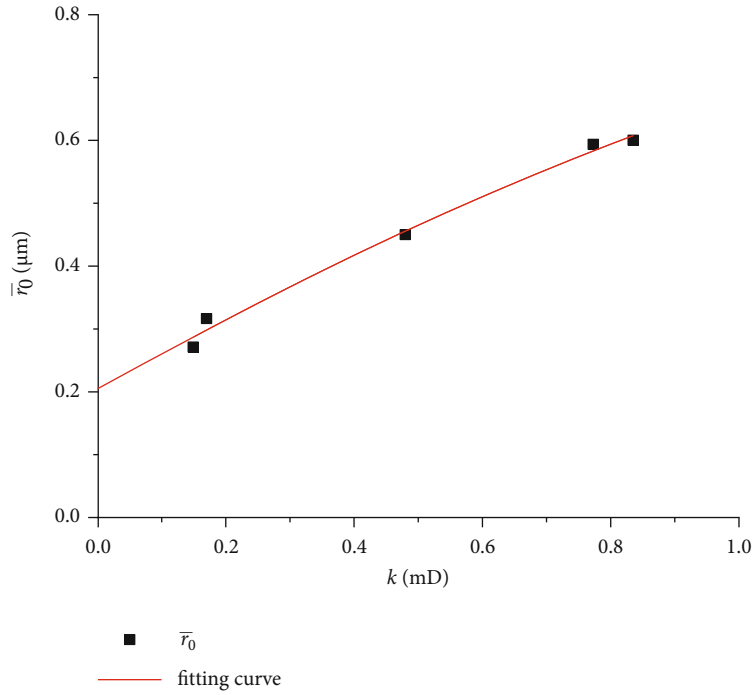

Figure 9: Relationship between average radius and permeability.

whole, which shows the flow characteristics of non-Newtonian fluid. The nonlinear fitting results can be divided into two stages: the nonlinear stage and the linear stage. When the displacement pressure is small, the flow velocity in the nonlinear section increases with the increase of the pressure gradient, and the slope of the curve gradually increases until it reaches linearity. The linear stage indicates that when water flows in the core, it is approximately Darcy seepage, and the velocity increases linearly with the increase of pressure gradient.

The error analysis of the pore size calculated by the theory and the pore size fitted by the experiment is shown in the following table. The error of the average pore size is less than 1%, indicating that the nonlinear phenomenon caused by the liquid flow is not caused by the measurement error, while it resulted from other factors such as the slip phenomenon at the micro- and nanoscale, as shown in Table 4. From the analysis of the nonlinear seepage mechanism of dense oil, the curve shows four main reasons for the nonlinear characteristics: (a) The water velocity and pressure gradient curve in porous media deviate from the Darcy law, which is because the influence of clay minerals makes the nature of the fluid become non-Newtonian. (b) Physical conditions such as fine pore throat and large specific surface area of porous media in tight cores lead to microscale flow effect of fluid flow in cores. (c) The phase behavior in nano-microporous media of tight oil reservoirs is different from that in conventional reservoirs. In nanopore space, the fluid phase behavior will change to some extent, thus changing the fluid characteristics. (d) The simulated formation water is mainly used in the experiment, which belongs to the polar fluid. Driven by the external pressure, the flow resistance increases and the electroviscous effect is produced.

Based on the above reasons, the possibility of nonlinear phenomenon caused by the measurement error is very small and can be almost ignored. It is mainly due to the influence of micro- and nanoscale effect. With the decrease of scale, the interaction between liquid-solid surfaces is more obvious and the stress sensitivity is enhanced, and the physical properties of reservoirs are changed. Therefore, the fluid shows the nonlinear seepage characteristics in the dense porous media.

4.3. Relationship between Core Permeability, Average Pore Radius, and Non-Newtonian Power-Law Coefficient n. Nonlinear fitting is carried out for the water velocity and pressure gradient in the cores to obtain the value of n and the average radius of the pores. The specific fitting values are shown in Table 5.

Average pore diameter of the experimental core is obtained from Table 5, establishing $\bar{r}_0$ and core permeability, as shown in Figure 9. It can be seen from Figure 9 that the larger the average pore radius of the tight core, the higher the permeability is. When water percolates in the dense core, it shows that the non-Newtonian power-law value n is not equal to 1, and its average value is 0.78. Because the permeability of the tight core in this experiment is similar, it is impossible to analyze the relationship between the non-Newtonian power-law coefficient n value of water flowing in the tight core and the permeability.

5. Conclusion

Based on the assumption of non-Newtonian fluid model of confined fluid in micro- and nanoscale, this study deduces the nonlinear seepage model of liquid, which provides a

new theoretical model for the study of the flow characteristics of liquid in micro-nanochannel and tight reservoirs.

(1) The diameter of channel, pressure gradient, and driving force are the main factors determining the characteristics of flow velocity curve. The displacement pressure gradient is less than 0.5 MPa, and the micro- and nanodiameter is in the nanometer scale, and the nonlinear characteristics of water flow in nanochannels are obvious;

(2) When deionized water flows in tight cores, the flow law conforms to the power-law nonlinear flow model. With the increase of the diameter, the non-Newtonian power-law parameter n is closer to 1 of Newtonian fluid.

Data Availability

Part of the data used in the manuscript to support the results of this study has been included in the article and supplementary information files. At present, the original/processed data required for these studies cannot be shared and copied, because these data are also part of the ongoing research and are true and effective. In order to prevent the disclosure of data information, all data cannot be provided free of charge. It is hereby declared.

Conflicts of Interest

The authors declare that they have no conflicts of interest.

Acknowledgments

This project is supported by the National Major Project of China (No. 2017ZX05072005) and by the National Natural Science Foundation of China (No. 11472246).

Supplementary Materials

Table S1: basic parameters of alumina film and micro-/nanocapillary. *(Supplementary Materials)*

References

[1] A. R. Rahmati and M. Derikvand, "Numerical study of non-Newtonian nano-fluid in a micro-channel with adding slip velocity and porous blocks," *International Communications in Heat and Mass Transfer*, vol. 118, p. 104843, 2020.

[2] Q. Gao, Y. Zhang, S. Xu et al., "Physicochemical properties and structure of fluid at nano-/micro-interface: progress in simulation and experimental study," *Green Energy & Environment*, vol. 5, no. 3, pp. 274–285, 2020.

[3] C. M. Ho and Y. C. Tai, "Micro-electro-mechanical-systems (MEMS) and fluid flows," *Annual Review of Fluid Mechanics*, vol. 30, no. 1, pp. 579–612, 1998.

[4] M. Gad-el-Hak, "The fluid mechanics of microdevices—the Freeman Scholar Lecture," *Journal of Fluids Engineering*, vol. 121, no. 1, pp. 5–33, 1999.

[5] H. Avdić and R. Šelo, "Continuum mechanics modeling of complex fluid systems following Oldroyd's seminal 1950 work," *Non-Newtonian Fluid Mechanics*, vol. 198, 2021.

[6] M. Makihara, K. Sasakura, and A. Nagayama, "The flow of liquids in micro-capillary tubes. Consideration to application of the Navier-Stokes equations," *Journal of the Japan Society for Precision Engineering*, vol. 59, no. 3, pp. 399–404, 1993.

[7] X. N. Jiang, Z. Y. Zhou, J. Yao, Y. Li, and X. Y. Ye, *Micro-Fluid Flow in Microchannel*, International Conference on Solid-state Sensors & Actuators. IEEE Xplore, 2004.

[8] V. M. Aniskin, K. V. Adamenko, and A. A. Maslov, "Experimental determination of the friction factor coefficient in microchannels," *Journal of Applied Mechanics and Technical Physics*, vol. 52, no. 1, pp. 18–23, 2011.

[9] S. M. Flockhart and R. S. Dhariwal, "Experimental and numerical investigation into the flow characteristics of channels etched in ⟨100⟩ silicon," *Journal of Fluids Engineering*, vol. 120, no. 2, pp. 291–295, 1998.

[10] Z. H. Li, X. B. Zhou, and S. N. Zhu, "Flow characteristics of non-polar organic liquids with small molecules in a microchannel," *Chinese Journal of Theoretical and Applied Mechanics*, vol. 34, no. 3, pp. 432–438, 2002.

[11] J. Judy, D. Maynes, and B. W. Webb, "Characterization of frictional pressure drop for liquid flows through microchannels," *International Journal of Heat and Mass Transfer*, vol. 45, no. 17, pp. 3477–3489, 2002.

[12] Z. X. Li, "Experimental study on flow characteristics of liquid in circular microtubes," *Microscale Thermophysical Engineering*, vol. 7, no. 3, pp. 253–265, 2003.

[13] B. Salman, H. A. Mohammed, A. S. H. Kherbeet, H. A. Mohammed, and A. S. Kherbeet, "Numerical and experimental investigation of heat transfer enhancement in a microtube using nanofluids," *International Communications in Heat and Mass Transfer*, vol. 59, pp. 88–100, 2014.

[14] S. L. Xu, X. A. Yue, and J. R. Hou, "Experimental study on flow characteristics of deionized water in micro circular tube [J]," *Chinese Science Bulletin (in Chinese)*, vol. 52, no. 1, pp. 120–124, 2007.

[15] A. Bucci, G. P. Celata, M. Cumo, E. Serra, and G. Zummo, "Water single-phase fluid flow and heat transfer in capillary tubes," *International Conference on Micro-channels and Mini-channel*, vol. 36673, pp. 319–326, 2003.

[16] G. P. Celata, M. Cumo, S. Mcphail, and G. Zummo, "Characterization of fluid dynamic behaviour and channel wall effects in microtube," *International Journal of Heat and Fluid Flow*, vol. 27, no. 1, pp. 135–143, 2006.

[17] Y. Liu, X. Dong, Z. Chen, Y. Hou, Q. Luo, and Y. Chen, "A novel experimental investigation on the occurrence state of fluids in microscale pores of tight reservoirs," *Journal of Petroleum Science and Engineering*, vol. 196, no. 1, p. 107656, 2021.

[18] Q. Lei, L. Zhang, H. Tang, Y. Zhao, M. Chen, and C. Xie, "Quantitative study of different patterns of microscale residual water and their effect on gas permeability through digital core analysis," *Journal of Petroleum Science and Engineering*, vol. 196, p. 108053, 2021.

[19] Z. H. A. O. Yulong, L. I. U. Xiangyu, L. Zhang, and S. H. A. N. Baochao, "A basic model of unconventional gas microscale flow based on the lattice Boltzmann method," *Petroleum Exploration and Development*, vol. 48, no. 1, pp. 179–189, 2021.

[20] F. Q. Song, L. W. Bo, H. Z. Gao, T. Dai, and Y. H. Sun, "Nonlinear percolation model for wetting fluid of tight reservoirs

based on micro-and nano-tubes flow characteristics," *Journal of Hydrodynamics*, vol. 34, no. 6, pp. 772–778, 2019.

[21] J. Judy, D. Maynes, and B. W. Webb, "Liquid flow pressure drop in microtubes," *International Conference on Heat Transfer and Transport Phenomena in Microscale*, pp. 149–154, 2000.

[22] Z. X. Li, D. X. Du, and Z. Y. Guo, "Experimental study on flow characteristics of liquid in circular microtubes," *International Conference on Heat Transfer and Transport Phenomena in Microscale*, pp. 162–167, 2000.

[23] P. X. Jiang, M. H. Fan, G. S. Si, and Z. P. Ren, "Thermal-hydraulic performance of small scale micro-channel and porous-media heat-exchangers," *International Journal of Heat and Mass Transfer*, vol. 44, no. 5, pp. 1039–1051, 2001.

[24] X. F. Peng, G. P. Peterson, B. X. Wang, G. P. Peterson, and B. X. Wang, "Frictional flow characteristics of water flowing through rectangular microchannels," *Experimental Heat Transfer*, vol. 7, no. 4, pp. 249–264, 1994.

[25] R. J. Jiang, F. Q. Song, and L. I. Hua-Mei, "Flow characteristics of deionized water in microtubes," *Chinese Physics Letters*, vol. 28, no. 10, pp. 3305–3308, 2011.

[26] F. Wang, X. A. Yue, S. L. Xu, L. J. Zhang, R. B. Zhao, and J. R. Hou, "Effect of wettability on flow characteristics of water through microtubes and cores," *Chinese Science Bulletin*, vol. 54, no. 13, pp. 2256–2262, 2009.

[27] F. Q. Song and L. Yu, "The boundary negative slippage of fluid flowing in wettability microtubes," *Journal of Hydrodynamics*, vol. 28, no. 2, pp. 128–134, 2013.

[28] Q. L. Chen, *Study on Heat Transfer Characteristics of Liquid Flow and Its Application in Micro Scale*, Zhejiang University, 2016.

[29] S. G. Kandlikar, "Fundamental issues related to flow boiling in minichannels and microchannels," *Experimental Thermal and Fluid Science*, vol. 26, no. 2-4, pp. 389–407, 2002.

[30] H. P. Fang, "The behavior of water transportation across nanometer sizechannels," *Physics*, vol. 40, no. 5, pp. 311–315, 2011.

[31] C. Zhang and Y. Chen, "Slip behavior of liquid flow in rough nanochannels," *Chemical Engineering and Processing Process Intensification*, vol. 85, pp. 203–208, 2014.

[32] S. C. Yang and L. B. Fang, "Effect of surface roughness on slip flows in hydrophobic and hydrophilic microchannels by molecular dynamics simulation," *Molecular Simulation*, vol. 31, no. 14-15, pp. 971–977, 2005.

[33] J. Shirai and K. Yoshida, "Water structure in 100 nm nanochannels revealed by nano X-ray diffractometry and Raman spectroscopy," *Journal of Molecular Liquids*, vol. 350, p. 118567, 2022.

[34] Z. Cheng, Z. Ning, and S. Dai, "The electroviscous flow of non-Newtonian fluids in microtubes and implications for nonlinear flow in porous media," *Journal of Hydrology*, vol. 590, no. 1-2, p. 125224, 2020.

[35] Z. Ling, Y. Liu, J. Ding, J. Yang, Z. Zhuang, and Z. Fan, "Experimental study on the characteristics of slip in hydrophilic and hydrophobic microchannels," *China Mechanical Engineering*, vol. 22, pp. 2326–2329, 2006.

[36] Z. Yu, X. Liu, and G. Kuang, "Water slip flow in superhydrophobic microtubes within laminar flow region," *Chinese Journal of Chemical Engineering*, vol. 23, no. 5, pp. 763–768, 2015.

[37] C. Qu and F. Q. Song, "Flow characteristics of deionized water in microtubes absorbing fluoro-alkyl silanes," *Chinese Physics Letters*, vol. 28, no. 10, p. 104701, 2011.

[38] J. Renjie, S. Fuquan, and L. Huamei, "Flow characteristics of deionized water in microtubes," *Chinese Physics Letters*, vol. 23, no. 12, pp. 3305–3308, 2006.

[39] S. Fuquan, J. Renjie, and B. Shuli, "Measurement of threshold pressure gradient of microchannels by static method," *Chinese Physics Letters*, vol. 24, no. 7, pp. 1995–1998, 2007.

[40] A. R. Rahmati, O. A. Akbari, A. Marzban, D. Toghraie, R. Karimi, and F. Pourfattah, "Simultaneous investigations the effects of non-Newtonian nanofluid flow in different volume fractions of solid nanoparticles with slip and no-slip boundary conditions," *Thermal Science and Engineering Progress*, vol. 5, pp. 263–277, 2018.

[41] X. Wang and J. J. Sheng, "Effect of low-velocity non-Darcy flow on well production performance in shale and tight oil reservoirs," *Fuel*, vol. 190, pp. 41–46, 2017.

[42] W. Z. Ye, X. Y. Wang, C. G. Cao, and W. S. Yu, "A fractal model for threshold pressure gradient of tight oil reservoirs," *Journal of Petroleum Science and Engineering*, vol. 179, pp. 427–431, 2019.

[43] N. I. N. G. Zhengfu, W. A. N. G. Bo, Y. A. N. G. Feng, Z. E. N. G. Yan, C. H. E. N. Jin'e, and L. Zhang, "Microscale effect of microvadose in shale reservoirs," *Petroleum Exploration and Development*, vol. 41, no. 4, pp. 492–499, 2014.

[44] L. Jun, "Non-deterministic method for tight oil reserves upgrade potential assessment and its application," *Oil & Gas Geology*, vol. 42, no. 3, pp. 755–764, 2021.

[45] H. U. Suyun, Z. H. U. Rukai, W. U. Songtao, B. A. I. Bin, Y. A. N. G. Zhi, and C. U. I. Jingwei, "Exploration and development of continental tight oil in China," *Petroleum Exploration and Development*, vol. 45, no. 4, pp. 790–802, 2018.

[46] C. Zou, Z. Yang, R. Zhu et al., "Geologic significance and optimization technique of sweet spots in unconventional shale systems," *Asian earth sciences*, vol. 178, pp. 3–19, 2019.

[47] S. Gao, Y. Yang, G. Liao et al., "Experimental research on inter-fracture asynchronous injection-production cycle for a horizontal well in a tight oil reservoir," *Journal of Petroleum Science and Engineering*, vol. 208, p. 109647, 2022.

[48] G. X. Li and R. K. Zhu, "Progress, challenges and key issues of unconventional oil and gas development of CNPC," *China Petroleum Exploration*, vol. 25, no. 5, pp. 1–13, 2020.

[49] Z. Rukai, Z. Caineng, W. Songtao et al., "Mechanism for generation and accumulation of continental tight oil in China," *Oil & Gas Geology*, vol. 40, no. 6, pp. 1168–1184, 2019.

[50] S. Fuquan, S. Xingxing, W. Yong, and S. Yeheng, "Single- and two-phase flow model in low-permeability reservoir," *Petroleum*, vol. 5, no. 2, pp. 183–190, 2019.

[51] Y. Wang, F.-q. Song, K. Ji, Y.-h. Sun, W.-y. Zhu, and X.-h. Wang, "Flow characteristics of silicon oil in nanochannels," *Hydrodynamics*, vol. 33, no. 6, pp. 1282–1290, 2021.

[52] R. C. Miao, J. W. Guo, L. Yang, Z. X. Chen, and M. Tao, "Molecular dynamics simulation of shear flow of nanofluids in microchannels," *Journal of Engineering Thermophysics*, vol. 41, no. 6, pp. 1477–1484, 2020.

[53] H. Esmaeilzadeh, J. Su, M. Charmchi, and H. Sun, "Effect of hydrophobicity on the water flow in carbon nanotube–a molecular dynamics study," *Theoretical and Applied Mechanics Letters*, vol. 8, no. 4, pp. 284–290, 2018.

[54] G. S. He and T. Hai, *Petrophysics*, Petroleum Industry Publishing House, Beijing, 2011.

[55] W. R. Purcell, "Capillary pressures - their measurement using mercury and the calculation of permeability

therefrom," *Journal of Petroleum Technology*, vol. 1, no. 2, pp. 39–48, 1949.

[56] S. Li, M. Dong, and P. Luo, "A Crossflow Model for an Interacting Capillary Bundle: Development and Application for Waterflooding in Tight Oil Reservoirs," *Chemical Engineering Science*, vol. 164, pp. 133–147, 2017.

[57] F. A. L. Dullien, "Effects of pore structure on capillary and Flo \v phenonlena in sandstones," *Journal of Canadian Petroleum Technology*, vol. 14, no. 3, pp. 48–55, 1975.

[58] S. Ren, F. Shen, S. Yang, X. Zhang, H. Luo, and C. Feng, "Analysis and calculation of threshold pressure gradient based on capillary bundle model," *Science Technology and Engineering*, vol. 16, no. 17, pp. 127–132, 2016.

[59] P. Liu, Z. Yuan, and K. Li, "An improved capillary pressure model using fractal geometry for coal rock," *Journal of Petroleum Science & Engineering*, vol. 145, pp. 473–481, 2016.

[60] X. Y. Kong, "Advanced seepage mechanics," *Hefei: Press of University of Science and Technology of China*, pp. 298–301, 2010.

[61] W. C. Liu, J. Yao, Z. X. Sun, and Z. Q. Huang, "Model of nonlinear seepage flow in low-permeability porous media based on the permeability gradual recovery," *Chinese Journal of Computational Mechanics*, vol. 29, no. 6, pp. 885–892, 2012.

[62] S. Fuquan, H. Xiao, Z. Genmin, and Z. Weiyao, "The characteristics of waterflow displaced by gas in nano arrays," *Chinese Journal of Theoretical and Applied Mechanics*, vol. 50, no. 3, pp. 553–560, 2018.

[63] W. Shen, F. Song, X. Hu, G. Zhu, and W. Zhu, "Experimental study on flow characteristics of gas transport in micro- and nanoscale pores," *Scientific Reports*, vol. 9, no. 1, p. 10196, 2019.